Use of the Fluorescence Detection System in Sedimentation Velocity Analytical Ultracentrifugation

Jia Ma, Huaying Zhao, Peter Schuck*

Dynamics of Macromolecular Assembly Section
Laboratory of Cellular Imaging and Macromolecular Biophysics
National Institute of Biomedical Imaging and Bioengineering
National Institutes of Health
Bethesda, Maryland

Abstract:
Sedimentation velocity analytical ultracentrifugation (SV-AUC) is a classic biophysical technique to determine the size and shape of macromolecules in solution, and to characterize their interactions with regard to the number, size, stoichiometry, and affinity of complexes formed in self-association and hetero-association processes. A recently introduced fluorescence detection system (FDS) extends the detection limit of SV-AUC by several orders of magnitude, permitting, for example, the study of binding events with picomolar dissociation constants. Further, the selectivity of fluorescence detection offers possibilities to apply SV to crowded solution such as biological fluids. The FDS system consists of an optics box, a switch box, a system box, and operating software. Data acquisition is controlled by several parameters including detector voltage and gain, focal depth of excitation beam, sector angle, and magnet angle. In this protocol, we demonstrate how to mount the FDS detector prior to an SV experiment, and how to adjust the required control parameters in the system software to initiate fluorescence data acquisition. Finally, we present FDS specific data pre-processing steps available in the SV data analysis software SEDFIT.

INTRODUCTION:

Sedimentation velocity (SV) analytical ultracentrifugation (AUC) experiments are based on the application of a gravitational field to a buffered solution of macromolecules, and the real-time measurement of the resulting macromolecular migration. The analysis of the evolution of sedimentation profiles in SV offers rich information on macromolecular mass, hydrodynamic shape, oligomeric state, and reversible protein interactions[1]. AUC is very versatile and has applications in many fields. For example, SV-AUC is widely used in the study of protein interactions, both for self- and hetero-association with two or more protein components[2,3]. After external calibration[4,5], absolute translational friction coefficients can be determined that can provide information on macromolecular structure in solution, which may be used to restrain models from small angle scattering[6], or be compared with structure-based hydrodynamic models [7–9]. In biotechnology, SV-AUC is frequently used as a tool to study aggregation propensity of protein pharmaceuticals in the development of formulations and for quality control[10,11].

Conventional optical detectors in current analytical ultracentrifuges are Rayleigh interference and absorbance detectors (permitting the acquisition of scans at multiple wavelengths in the same experiment)[12,13]. These enable the detection of proteins in the low µg/ml range [13,14]. This sensitivity is far surpassed with fluorescence detection[15–17] using a recently introduced commercial detector for current AUC instruments (FDS, AVIV Biomedical, Inc.). It has a confocal design with 488 nm excitation and emission detection between 505 and 565 nm. FDS-SV has been demonstrated to detect macromolecules at concentrations below 3 pM FITC-labeled BSA[18] and 1 pM EGFP[19]. Besides lowering the required amount of protein, this allows the quantitative study of protein interactions with significantly higher affinity [14,19–22], with dissociation constants ranging into the low picomolar range[19], and the qualitative and comparative study of proteins in crowded solutions such as cell extracts and serum[18,21,23–26]. Characteristics of FDS prototypes have been previously described[17,27]; the performance of the commercial instrument has been recently studied in detail with regard to the impact of photobleaching and other induced photophysical processes[28], inner filter effect and signal linearity[29,30], characteristic signal offsets[30], considerations for labeling and the prevention of surface adsorption[20]. Suitable computational tools for data analysis have been incorporated in the software SEDFIT[31].

The general strategy and experimental protocol for using fluorescence-detected SV-AUC is in many ways similar to that of the conventional optical detectors, which has been described in detail previously[13,32]. Here, we show the experimental steps specific for setting up the FDS detector in SV-AUC.

PROTOCOL:

Fluorescence detected AUC requires an Optima XL-A/I analytical ultracentrifuge (Beckman Coulter, Indianapolis, IN) retrofitted with the FDS (AVIV Biomedical Inc, Lakewood, NJ). For quantitative results, external temperature calibration of the AUC using iButton is recommended.[33,34] The procedures listed below apply to recent FDS systems with either a 10 mW solid-state laser or a 50 mW diode laser. For some of the steps, alternative procedures are possible, but the steps described below are established and successfully used in our laboratory using a system with solid state laser and the AOS version 2.1.0.0.

1. Sample cell preparation

1.1) Calibration cell

The FDS requires a calibration cell which is used by the system for radial and angular calibration. It has a centerpiece with a central rectangular channel loaded with 40 µL of 10 µM fluorescein in Tris buffer (100 mM KCl, 10 mM TRIS, pH 7.8)[35]. In this protocol, we use an eight hole-rotor with the calibration cell in the position #4 (which can be assigned by the user).

1.2) Sample cells

The FDS-AUC uses the standard procedures for the assembly of sample cells, which are fully explained in our previous video protocol[32]. However, the fluorescence detection system does not need a blank buffer sector as a reference. Therefore, both sectors of a double-sector centerpiece can be loaded with different samples. To differentiate two sectors, the AVIV FDS system refers to the left sector (top view into the cell with filling holes pointing away – conventionally the reference sector) as the sector A and the right sector (conventionally the sample sector) as the sector B.

It is best to arrange samples such that they are paired in the same cells to produce similar fluorescence intensities.

Note: It is critically important that sample cell assemblies have been meticulously cleaned. Due to the higher sensitivity of FDS compared to conventional optical detection, dependent on the molecules under study and the concentration used, more stringent cleaning procedures may be required than usual; this may be verified by running in the FDS some cell assemblies filled with water.

1.3) Rotor set-up

Up to 14 samples can be loaded in one run using the 8-hole rotor. Balance and align all cells in the rotor. Place the rotor onto the drive spindle in the rotor chamber.

2. Set-up of FDS

2.1) Mounting the optics box

While not in use, the FDS optics box should be kept on a storage base plate with a white plastic dust cover slipped on to protect the focusing lens. The white plate dust cover should be firstly pulled out of the optics box and kept in a safe place. The optics box is removed from the storage base plate by unscrewing two thumb screws on the mounting bracket and gently lifting the box from the base plate, while preventing the box from sliding along the internal rail. When holding the optic box, one should avoid touching the focusing lens. The optics box is connected with the FDS through the electrical connector in the AUC chamber. The optics box is mounted by first aligning it with the guided posts on the mounting bracket and then lowering it onto the electrical connector. Only if properly aligned, a gentle pressure on the mating bracket (but not the optics box) may be applied to help to establish a secure fit. The box and the electrical connector are fixed in place by using a large screw driver to tighten two thumb screws. At this stage, the rotor chamber should be left open.

2.2) Power on FDS system

2.2.1) Prior to activation of the FDS system, electronic connections for centrifuge control need to be rerouted from the computer used for the control of the Beckman absorbance and interference detectors to connect to the FDS control computer. For this purpose, a switch box is used, which should be switched into the "A" position for the FDS system.

2.2.2) After the computer controlling the AVIV system is turned on, the black system box can be turned on. The yellow top light in the system box indicates it is powered up. Two red lights on the top of the optics box also should be on. If not, please turn off the system box and check the connection between the optics box and the electrical connector.

2.2.3) After checking all settings, close the centrifuge chamber and turn on vacuum. Select a rotor speed of 0 rpm and press "START" at the centrifuge console.

2.2.4) The whole system should now be temperature equilibrated as usual at the target temperature for at least two hours.[13]

3. Software set-up of FDS control and data acquisition parameters

3.1) System initiation

3.1.1) The "advanced operating system" software (AOS) is used in the AVIV FDS to control the centrifuge and to acquire data. To start AOS, double-click the AOS icon on the desktop. A window appears and asks to confirm the location of the calibration cell and rotor setup. Please check whether the location of the calibration cell is right or not. If it is, click OK and the system initiates.

3.1.2) In AOS, an optical system status box shows the status of fluorescence, FDS laser, centrifuge power, interface power, and magnet angle. At this stage, the fluorescence, centrifuge power, and interface power are on with the green light. The FDS laser is initiating with the yellow light. When the vacuum goes below 170 microns, the laser turns on automatically, and the corresponding light turns from yellow to blue, which indicates the laser

is warming up. When the color changes from blue to green, the laser is ready to use. The magnet angle is white and not available in this step.

3.1.3) The AVIV system communicates with the centrifuge and the machine status bar shows that the machine is running (since temperature equilibration was carried out with the rotor 'running' at 0 rpm). If the centrifuge is not running yet, the instrument can be started by clicking the start menu and only checking the box "start machine". Keep the rotor speed at 0 rpm. If the centrifuge is running already, the step of "start machine" is not required.

3.2) Experiment set-up

An experimental run can be set up by Wizard button step by step. Click the Wizard button in AOS.

3.2.1) Button 1: Logon to the system by your username and password.

3.2.2) Button 2: Input the experimental information. Name your experiment and select a folder path to store your data. You can also set up your running parameters in this step.

3.2.3) Button 3: Specify the position of the calibration cell. In this demonstration, the calibration cell is loaded in the fourth position in an eight-hole rotor.

3.2.4) Button 4: Determine the duration, rotor speed, and temperature of this run. You can select a stored method or create a new one. To create a new method, click the new method button. In the new method creation panel, the temperature, rotor speed, and scanning parameters need to be specified.

3.2.5) Button 5: Select the cells to be scanned by checking the cell number. Deselect rotor positions that do not have samples, by checking the square in from the cell number.

3.3) Magnet angle lock

Locking the magnet angle is the process in which the FDS synchronizes the rotor movement with the data acquisition and identifies which sector is in the FDS laser light path at any point in time. It requires that the laser is on and warmed up (indicator light green).

3.3.1) Now the rotor can be accelerated by inputting the target speed in the centrifuge console. When the speed reaches the target, the magnet angle light turns yellow indicating the magnet angle determination is in process.

3.3.2) Observe the magnet angle light: When the magnet angle is locked, the light will change to green.

Troubleshooting: If the magnet angle failed to lock with a white indicator light, this means the laser is not ready. In this case the laser will need to be engaged and warmed up. Otherwise, if the laser is ready but the magnet angle failed to lock, check the fluorescence intensity of the calibration cell: By clicking the fluorescence option from the fluorescence menu, the focusing and calibration tool panel appears. The fluorescence intensity of the calibration cell should be

around 1000 counts. If the intensity is too low, the magnet angle cannot be locked. Adjust the fluorescence intensity of the calibration cell by selecting a suitable photomultiplier voltage, and a suitable focal depth. Then re-initiate this step by clicking the "Force Magnet Angle" option from the hardware menu.

3.4) Fluorescence intensity

To obtain proper signal-to-noise ratios for the data, the fluorescence intensity of samples should be adjusted by the voltage of a photomultiplier (PMT) tube and the amplifier gain. Click the "Set Gain" option from the fluorescence menu. The fluorescence intensity of each cell can be adjusted by clicking the cell number and change the value of voltage and gain while monitoring the approximate fluorescence intensity values displaying on the bar graph. The following considerations apply:

- Normally, the fluorescence intensity should be between 500 counts to 3500 counts.
- It is desirable to bring all signals into this range with the fewest gain/voltage combinations, in order obtain the highest possible frequency of scans.
- In order to allow quantitative comparison of total signals across different cells, since the signal is non-linear in PMT voltage, they need to be scanned with at least one shared voltage setting (adjusting signal levels with gains).
- For the time intervals between scans, the limiting is the number of different PMT voltage/gain combinations required, but not the number of cells scanned at each condition. Therefore, it is useful to acquire data from all cells at all voltage/gain combinations. This will record a lot of data, but the data files can be sorted with the SEDFIT tool later.

3.5) Sector angles

The rotational angle during which illumination and fluorescence acquisition occurs should be well within the sample sectors for each cell.

To set up the sector angles, click the centerpiece button in the AOS menu bar. In the panel that appears, select the cell and the sector. A graph of fluorescence intensity versus angular position appears. In the graph, two stationary black lines display the scanning region and wobbly lines indicate the fluorescence signal refreshing in real-time. Elevated noise occurs if the scanning region overlaps with the edges of the fluorescence signal. To avoid overlap, change the angle offset by sliding the angle bar on the left, and adjust the duration of acquisition.

4. Radial scanning

4.1) Initiate acquisition

When the fluorescence signal is adjusted, the experiment is ready to start. Click the start button again. Check "start experiment" this time. Choose "No" to reset it to 0 rpm, to avoid ill-defined sedimentation conditions arising from stop/re-start cycle. (If the user inadvertently clicked "Yes" and the centrifuge went back to 0 rpm, then sample cells should be taken out, and the

samples should be gently remixed by inverting cells several times. The rotor should then temperature re-equilibrated two hours at the target temperature.)

4.2) Start acquisition

Click the "manual start", and the FDS starts to scan the cells. Acquired data are displayed in the scan window. Proceed with the run until sedimentation experiment and/or the scan protocol is completed.

5. AOS exit and system power off

The AOS can be closed by clicking the file menu and selecting exit option. It is important to exit the program properly after the experiment so the optical parts can be homed. Save everything and click OK. After closing AOS, turn off the system box. Stop the AUC and release the vacuum.

The optical box should be removed by unscrewing the two thumb screws and lifting it up from the electrical connector. The optical box mounted back onto the storage plate and the dust cover should be replaced.

6. Data sorting and analysis

6.1) Sorting

Thousands of scan files can be generated by the AOS in a single FDS-SV experiment. All original scan files have a label of sector at the beginning of the filenames followed by the scan number. While it is easy to identify the sector, it is difficult to distinguish scans from different PMT voltage/gain settings. This is greatly facilitated in a SEDFIT function.

6.1.1) Load a subset of original fluorescence scan files data into SEDFIT, and choose the "Sorting Fluorescence Data to Disk" from the fluorescence tools selection under the options menu. This will start processing the data in the selected directory and copy the sorted data with an expanded filename into a new subfolder named "sorted".

6.1.2) It is possible to make lists of files ready for data analysis in SEDFIT. Criteria for inclusion in these lists can be established according to time-intervals of scans, target number of scans to include, and a signal threshold filter. This will sort the files and create list-files that can be directly loaded in SEDFIT.

6.2) Analysis

Detailed advice on the analysis of SV data is outside the scope of this protocol. Generally, the same principles as for conventionally detected SV data should be applied.[13] The most commonly applied model is the sedimentation coefficient distribution c(s)[36].

Unique data features of FDS data include temporal signal intensity drifts, radial-dependent signal magnification gradients, and artifacts from partially obscured beams at the bottom of the cell, as described in detail previously[30]. Corrections for these effects are superimposed to the

standard models, and can be switched with the keyboard shortcut ALT-F (or in the "Fluorescence Tool" Options menu).

7. Optional steps: meniscus localization, radial calibration, and focus adjustment

7.1) Observe meniscus position

Optionally, prior to exiting the system, it is possible to locate the meniscus position through the step in baseline signal at the air/solvent interface caused by Raman scattering[19]. This is possible with equipment using either a 10 mW or 50 mW laser.

7.1.1) While the rotor is still spinning at full speed, stop data acquisition and elevate the PMT voltage to a high level.

7.1.2) Restart data acquisition, and observe the resulting scan data for the step in the baseline in the radial range where the meniscus is expected (~ between 5.9 cm and 6.1 cm for a standard double sector centerpiece filled with 400 µL sample in each sector).

7.2) Radial calibration

From time to time, the AU-FDS needs to be radially calibrated to function properly and produce reliable data. The radial calibration should be performed using the calibration cell, and at low rotor speed (at or below 5,000 rpm) to avoid the stretch of rotor at a higher speed.

7.2.1) To start a radial calibration, choose the speed to 3,000 rpm, initiate AOS and lock the magnet angle as usual, but do not start collecting scans.

7.2.2) Click the fluorescence panel from the fluorescence focusing menu. The focusing and calibration tool windows pops up. Firstly check the fluorescence intensity of the calibration cell. In the upper right, the detector gain control can adjust the PMT voltage to have fluorescence intensity around 1000. To perform the radial calibration, click the radial scan button. The AOS will automatically scan the cell from the bottom to the top. The user can save new parameters by clicking the Save Radial Cal button.

7.3) Focus scan

A focus scan is a scan of a sample solution at fixed radius into the z-direction perpendicular to the plane of rotation. Optionally, it can be carried out, prior to the fluorescence intensity adjustments of each sample cell and the calibration cell.

7.3.1) With the centrifuge running, initiate AOS and lock the magnet angle as usual, but do not start scans.

7.3.2) Click the fluorescence panel from the fluorescence focusing menu. The focusing and calibration tool window appears. Select a sample cell from the "calibration cell location" box. Then, in the upper left focal settings box, select the desired radius (usually in the middle of the solution column for the target sample). If necessary, adjust the PMT voltage to ensure a signal

between 1,000 to 3,000 counts. To perform a focus scan, just click the Focus Scan button. When a focus scan is finished, a plot of intensity versus focal depth is displayed.

7.3.3) Adjust the focus using the following considerations:

- Small focal depths (1,000 – 2,000 µm) are optimal to minimize the region of radial artifacts near the meniscus and bottom. Usually there is a strong slope in the focal scan in this range, and, dependent on the particular instrument, the focal depth-dependence of the signal may produce radial-dependent signal magnification gradients. These can be accounted for computationally (Fluorescence Tools in SEDFIT).[30]
- Large focal depths (5,000 µm and above) typically have a declining slope in the focal scan, and may promote inner filter effects causing non-linear signals for higher concentrated samples. They also exacerbate the radial range of optical artifacts close to either end of the solution column.
- Intermediate focal depths (~ 3,000 – 4,000 µm) are frequently used as a compromise. There is no need to be on the maximum of the focal scan curve[30].

7.3.4.) Save the new parameters by clicking the Save Focus button.

7.3.5) Make sure the photomultiplier voltages will be re-adjusted for each sample and the calibration cell (Step 3.4 above).

REPRESENTATIVE RESULTS

It may be useful to carry out control experiments in order to assess successful application of this protocol. EGFP is particularly suitable as an ubiquitously available model protein, and results can be compared with published data.[30] A set of fluorescence scans of EGFP is shown in Figure 1.

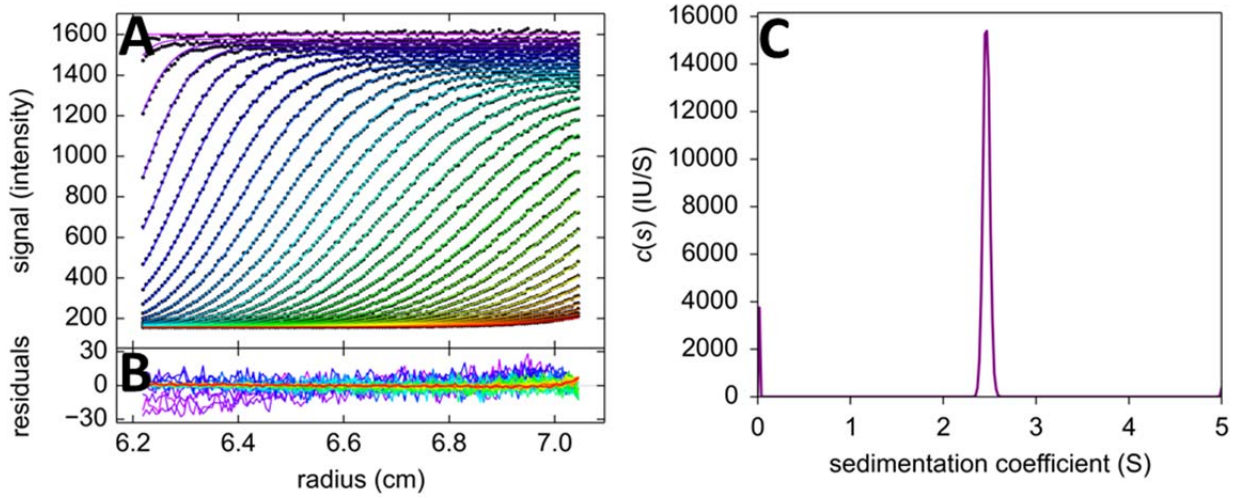

Figure 1: Panel A: Representative FDS-SV data from the sedimentation of 100 nM EGFP in phosphate buffered saline (1.06 mM KH_2PO_4, 154.00 mM NaCl, 5.60 mM Na_2HPO_4, pH 7.4) at 50,000 rpm, 19.29 °C. The solid line is the best-fit with the c(s) model[36]. Panel B: Residuals of

the fit. Panel C: c(s) distribution from the analysis of the data in A, with peak integration leading to a s_w-value after viscosity correction to water 20 °C of 2.51 S.

DISCUSSION

The fluorescence detection extends the dynamic range of AUC experiments by several orders of magnitude. This allows both the study of samples that are too scarce to achieve concentration and volume requirements of absorbance or interference detection, as well as the study of interacting systems at sufficiently low concentrations for dissociation of high-affinity complexes to occur, allowing the reliable determination of the binding constants[14,19–22]. In addition, the selectivity of the detection has the potential for studying macromolecular sedimentation in complex solutions, such as cell extract or serum[18,21,23–26].

Studies in complex solvents are complicated by multi-component non-ideal sedimentation, and, in view of lacking theoretical models, only semi-empirical or comparative characterizations seem possible. By contrast, the use of fluorescence detection for dilute solutions provides data that are highly quantitative and can be interpreted rigorously.[30] In fact, after computationally accounting for FDS-specific data characteristics, such as spatial and temporal signal magnification gradients, the data quality is superb and rivals that of the interference optical detection.[30] Inner filter effects, quenching, and/or photo-conversion of fluorophores are usually not encountered with ordinary fluorophores in dilute solutions[28,30].

This video for the FDS setup demonstrates that the routine use of FDS is quite straightforward, despite the additional control parameters involved. Some more thought must be given to buffer conditions when working with sub-nanomolar concentrations in dilute solutions, since the addition of an inert blocking agent (such as kappa-casein[19]) is usually required to prevent surface adsorption of the protein of interest. Further, if proteins are not expressed as fusion with fluorescent proteins, external labeling may be required, which adds potential complications in the sample preparation[20]. These steps will usually necessitate additional control experiments. Fortunately, the amount of sample is typically not critical at these low concentrations, and the high number of samples that can be run side-by-side facilitates such controls.

Acknowledgments:

This work was supported by the Intramural Research Program of the National Institute of Biomedical Imaging and Bioengineering, National Institutes of Health.

References:

1. Lebowitz, J., Lewis, M. S. & Schuck, P. Modern analytical ultracentrifugation in protein science: a tutorial review. *Protein science : a publication of the Protein Society* **11** (9), 2067–2079, doi:10.1110/ps.0207702 (2002).

2. Harding, S. E. & Rowe, A. J. Insight into protein-protein interactions from analytical ultracentrifugation. *Biochem. Soc. Transact.* **38** (4), 901–7, doi:10.1042/BST0380901 (2010).

3. Schuck, P. Analytical ultracentrifugation as a tool for studying protein interactions. *Biophys. Rev.* **5** (2), 159–171, doi:10.1007/s12551-013-0106-2 (2013).

4. Zhao, H., Ghirlando, R., *et al.* A multilaboratory comparison of calibration accuracy and the performance of external references in analytical ultracentrifugation. *PloS one* **10** (5), e0126420, doi:10.1371/journal.pone.0126420 (2015).

5. Ghirlando, R., Balbo, A., *et al.* Improving the thermal, radial, and temporal accuracy of the analytical ultracentrifuge through external references. *Anal. Biochem.* **440** (1), 81–95, doi:10.1016/j.ab.2013.05.011 (2013).

6. Perkins, S. J., Nan, R., Li, K., Khan, S. & Abe, Y. Analytical ultracentrifugation combined with X-ray and neutron scattering: Experiment and modelling. *Methods* **54** (1), 181–99, doi:10.1016/j.ymeth.2011.01.004 (2011).

7. Rai, N., Nöllmann, M., Spotorno, B., Tassara, G., Byron, O. & Rocco, M. SOMO (SOlution MOdeler) differences between X-Ray- and NMR-derived bead models suggest a role for side chain flexibility in protein hydrodynamics. *Structure* **13** (5), 723–734, doi:10.1016/j.str.2005.02.012 (2005).

8. Aragon, S. R. Recent advances in macromolecular hydrodynamic modeling. *Methods* **54** (1), 101–14, doi:10.1016/j.ymeth.2010.10.005 (2011).

9. Ortega, A., Amorós, D. & García de la Torre, J. Prediction of hydrodynamic and other solution properties of rigid proteins from atomic- and residue-level models. *Biophys. J.* **101** (4), 892–8, doi:10.1016/j.bpj.2011.06.046 (2011).

10. Berkowitz, S. A. & Philo, J. S. Characterizing biopharmaceuticals using analytical ultracentrifugation. *Biophysical Characterization of Proteins in Developing Biopharmaceuticals* , 211–260, doi:10.1016/B978-0-444-59573-7.00009-9 (2015).

11. Gabrielson, J. P. & Arthur, K. K. Measuring low levels of protein aggregation by sedimentation velocity. *Methods* **54** (1), 83–91, doi:10.1016/j.ymeth.2010.12.030 (2011).

12. Balbo, A., Minor, K. H., Velikovsky, C. A., Mariuzza, R. A., Peterson, C. B. & Schuck, P. Studying multi-protein complexes by multi-signal sedimentation velocity analytical ultracentrifugation. *Proc. Nat. Acad. Sci. USA* **102** (1), 81–86, doi:10.1073/pnas.0408399102 (2005).

13. Zhao, H., Brautigam, C. A., Ghirlando, R. & Schuck, P. Current methods in sedimentation velocity and sedimentation equilibrium analytical ultracentrifugation. *Curr. Protoc. Protein Sci.* **7**, 20.12.1, doi:10.1002/0471140864.ps2012s71 (2013).

14. Zhao, H., Berger, A. J., *et al.* Analysis of high-affinity assembly for AMPA receptor amino-terminal domains. *J. Gen. Physiol.* **139** (5), 371–388, doi:10.1085/jgp.201210770 (2012).

15. Schmidt, B., Rappold, W., Rosenbaum, V., Fischer, R. & Riesner, D. A fluorescence detection system for the analytical ultracentrifuge and its application to proteins, nucleic acids, and viruses. *Colloid & Polymer Science* **268** (1), 45–54, doi:10.1007/BF01410422 (1990).

16. Crepeau, R. H., Conrad, R. H. & Edelstein, S. J. UV laser scanning and fluorescence monitoring of analytical ultracentrifugation with an on-line computer system. *Biophys. Chem.* **5** (1-2), 27–39, doi:10.1016/0301-4622(76)80024-5 (1976).

17. MacGregor, I. K., Anderson, A. L. & Laue, T. M. Fluorescence detection for the XLI analytical ultracentrifuge. *Biophys. Chem.* **108** (1-3), 165–185, doi:10.1016/j.bpc.2003.10.018 (2004).

18. Le Roy, A., Wang, K., Schaack, B., Schuck, P., Breyton, C. & Ebel, C. AUC and Small-Angle Scattering for Membrane Proteins. *Methods Enzymol.* , doi:10.1016/bs.mie.2015.06.010 (2015).

19. Zhao, H., Mayer, M. L. & Schuck, P. Analysis of protein interactions with picomolar binding affinity by fluorescence-detected sedimentation velocity. *Anal. Chem.* **18** (6), 3181–3187, doi:10.1021/ac500093m (2014).

20. Zhao, H., Lomash, S., Glasser, C., Mayer, M. L. & Schuck, P. Analysis of high affinity self-association by fluorescence optical sedimentation velocity analytical ultracentrifugation of labeled proteins: opportunities and limitations. *PLoS ONE* **8** (12), e83439, doi:10.1371/journal.pone.0083439 (2013).

21. Kingsbury, J. S. & Laue, T. M. Fluorescence-detected sedimentation in dilute and highly concentrated solutions. *Methods Enzymol.* **492**, 283–304, doi:10.1016/B978-0-12-381268-1.00021-5 (2011).

22. Rossmann, M., Sukumaran, M., Penn, A. C., Veprintsev, D. B., Babu, M. M. & Greger, I. H. Subunit-selective N-terminal domain associations organize the formation of AMPA receptor heteromers. *EMBO J.* **30** (5), 959–71, doi:10.1038/emboj.2011.16 (2011).

23. Mok, Y.-F., Ryan, T. M., Yang, S., Hatters, D. M., Howlett, G. J. & Griffin, M. D. W. Sedimentation velocity analysis of amyloid oligomers and fibrils using fluorescence detection. *Methods* **54** (1), 67–75, doi:10.1016/j.ymeth.2010.10.004 (2011).

24. Olshina, M. A., Angley, L. M., *et al.* Tracking mutant huntingtin aggregation kinetics in cells reveals three major populations that include an invariant oligomer pool. *The Journal of biological chemistry* **285** (28), 21807–21816, doi:10.1074/jbc.M109.084434 (2010).

25. Demeule, B., Shire, S. J. & Liu, J. A therapeutic antibody and its antigen form different complexes in serum than in phosphate-buffered saline: A study by analytical ultracentrifugation. *Anal. Biochem.* **388** (2), 279–287, doi:10.1016/j.ab.2009.03.012 (2009).

26. Hill, J. J. & Laue, T. M. *Protein Assembly in Serum and the Differences from Assembly in Buffer*. *Methods Enzymol.* , doi:10.1016/bs.mie.2015.06.012 (Elsevier Inc.: 2015).

27. Kroe, R. R. & Laue, T. M. NUTS and BOLTS: Applications of fluorescence-detected sedimentation. *Anal. Biochem.* **390** (1), 1–13, doi:10.1016/j.ab.2008.11.033 (2009).

28. Zhao, H., Ma, J., *et al.* Accounting for photophysical processes and specific signal intensity changes in fluorescence-detected sedimentation velocity. *Analytical chemistry* **86** (18), 9286–9292, doi:10.1021/ac502478a (2014).

29. Lyons, D. F., Lary, J. W., Husain, B., Correia, J. J. & Cole, J. L. Are fluorescence-detected sedimentation velocity data reliable? *Analytical biochemistry* **437** (2), 133–137, doi:10.1016/j.ab.2013.02.019 (2013).

30. Zhao, H., Casillas, E., Shroff, H., Patterson, G. H. & Schuck, P. Tools for the quantitative analysis of sedimentation boundaries detected by fluorescence optical analytical ultracentrifugation. *PLoS ONE* **8** (10), e77245, doi:10.1371/journal.pone.0077245 (2013).

31. Schuck, P. https://sedfitsedphat.nibib.nih.gov/software/default.aspx. (2010).

32. Balbo, A., Zhao, H., Brown, P. H. & Schuck, P. Assembly, loading, and alignment of an analytical ultracentrifuge sample cell. *Journal of visualized experiments : JoVE* (33), e1530, doi:10.3791/1530 (2009).

33. Zhao, H., Balbo, A., Metger, H., Clary, R., Ghirlando, R. & Schuck, P. Improved measurement of the rotor temperature in analytical ultracentrifugation. *Analytical biochemistry* **451**, 69–75, doi:10.1016/j.ab.2014.02.006 (2014).

34. Ghirlando, R., Zhao, H., *et al.* Measurement of the temperature of the resting rotor in analytical ultracentrifugation. *Analytical biochemistry* **458**, 37–39, doi:10.1016/j.ab.2014.04.029 (2014).

35. *Analytical ultracentrifuge fluorescence detection system and advanced operating system user manual.* (AVIV Biomedical Inc: Lakewood, NJ, 2009).

36. Schuck, P. Size-distribution analysis of macromolecules by sedimentation velocity ultracentrifugation and Lamm equation modeling. *Biophys. J.* **78** (3), 1606–1619, doi:10.1016/S0006-3495(00)76713-0 (2000).